



Levenberg-Marquardt's and Gauss-Newton algorithms for parameter optimisation of the motion of a point mass rolling on a turntable

Soufiane Haddout^a and Mbarek Rhazi^b

^aFaculty of Science, Department of Physics, Ibn Tofail University, Kenitra, Morocco; ^bDepartment of Physics, ENS-Marrakech, Marrakech, Morocco

ABSTRACT

The problem of a point mass in a rotating system subjected to inertial force is theoretically and analytically solved, to get a more complete understanding of the different scenarios of motion in rotating system with friction being neglected. Subsequently, the solution is quantitatively verified by experimental data, solving non-linear least squares problems, based on Levenberg–Marquardt's and Gauss–Newton methods by minimising the sum of squares of errors between the data and model prediction. The process of model fitting is closely related to parameter identification. The optimisation parameters of the model (initial velocity of a point mass and angular velocity) are estimated. Experimental observation of the trajectories of a point mass rolling on a turntable is analysed from a video capture webcam in a mechanics laboratory. A good fit of the theoretical study with experimental data using optimisation methods output shows that there are instruments to directly verify rather abstract mechanical formulation in a non-inertial frame. It also demonstrates that a relatively simple theoretical background can be used for describing real different types of motion in mechanics and for explaining experimental results. Moreover, combining the theoretical description of the problem with experimental data and computational optimisation procedures gives a very easy understanding of the different scenarios of motion in a rotating system and parameters identification, which can be obtained in classical mechanics. On the other hand, this study represents an important and instructive topic in classical mechanics that cannot be omitted in physical modelling on the undergraduate university level.

ARTICLE HISTORY

Received 6 September 2015
Accepted 9 May 2016

KEYWORDS

Classical mechanics; laboratory experiment; point mass; motion; optimisation parameters; Levenberg–Marquardt's and Gauss–Newton methods

Introduction

The study of point mass motion in rotating frames is a crucial part of an undergraduate mechanics course (Agha, Gupta, & Joseph, 2015). This motion is generally

explained by invoking inertial forces and introduces many complex features. While this approach simplifies some problems, there is often little physical insight into the motion, in particular into the effects of the Coriolis force (McIntyre, 2000). Fundamentally, the acceleration of the rotating observer causes motion that is well behaved as viewed by an inertial observer to become distinctly non-intuitive when viewed by the rotating observer. The inertial forces are fictitious forces that arise in the description of the motion of test particles when the reference frame is not inertial (Costa & Natário, 2015; Kim, Kido, Rangel, & Madou, 2008; Taylor, 1974; Wagner, Altherr, Eckert, & Jodl, 2006). These forces do not exist; they are invented to preserve the Newtonian world view in reference systems where it does not apply (Kirkpatrick & Francis, 2009). Centrifugal and Coriolis forces arise in rotating reference systems (i.e. that are accelerated) and are examples of inertial forces. For instance, a point mass is launched directly away from the centre of the rotating turntable. The point mass will be rolling without forces acting on it; therefore its trajectory of motion is a straight line (path relative to laboratory reference) if we neglect friction and a path curved to the right on the rotating turntable surface (from the view of the rotating reference system) (Persson, 2000a, 2000b) (See Figure 1).

An observer standing next to the rotating turntable sees the point mass rolling straight and the rotating turntable rotate at angular velocity ω underneath it. In the accelerated coordinate system, we explain the apparent curve to the right using a fictitious force, called the Coriolis force that causes the point mass to curve to the right (Persson, 2000a, 2000c).

In other hand, the inertial force study is the key to the explanation of many phenomena in connection with the winds (e.g. the Coriolis effect is that wind directions in the Northern Hemisphere are deflected to the right, while those in the Southern Hemisphere are deflected to the left) and currents of the ocean. The cause of the Coriolis effect is the earth's rotation. Those phenomena are crucial to any analysis of weather systems and the large-scale climatology of the earth. The use of a rotating frame can also simplify the study of certain mechanics problems that involve rotating bodies in the laboratory.

The general approach in model fitting is to select a merit or objective function that is a measure of the agreement between observed and modelled data, and which is directly or indirectly related to the adjustable parameters to be fitted. The goodness of fit parameters are obtained by minimising (or maximising, depending on how the function is defined) this objective function (Simuunek & Hopmans, 2000). Many techniques have been developed to solve the non-linear minimisation or maximisation problem (Bard, 1970; Yeh, 1986). Most of these methods are iterative algorithms (e.g. Levenberg–Marquardt's, Gauss–Newton, gradient descent ... etc.) used to solve non-linear least squares problems.

The Levenberg–Marquardt's method is actually a combination of two minimisation methods: the gradient descent method and the Gauss–Newton method (Haddout, Maslouhi, & Igouzal, 2015). In the gradient descent method,

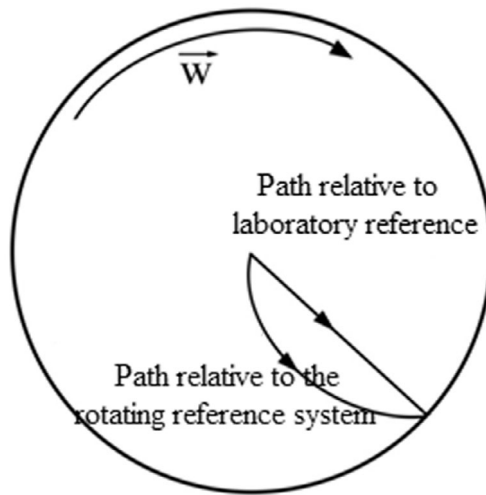


Figure 1. To the stationary observer, the ball follows a straight-line path, so the observer in the rotating frame system is forced to invoke a combination of centrifugal and Coriolis forces to provide the net force required to cause the curved trajectory.

the sum of the squared errors is reduced by updating the parameters in the direction of the greatest reduction of the least squares objective (Gavin, 2011). In the Gauss–Newton method, the sum of the squared errors is reduced by assuming the least squares function is locally quadratic, and finding the minimum of the quadratic. The Levenberg–Marquardt’s method acts more like a gradient descent method when the parameters are far from their optimal value, and act more like the Gauss–Newton method when the parameters are close to their optimal value (Gavin, 2011).

In the presented paper, a problem of a point mass in a rotating system subjected to inertial force is theoretically and analytically solved, to get a more complete understanding of the different types of motion of point mass with respect to a non-inertial reference frame using Maple and Matlab programmes. Additionally, the non-linear model fitting of the motion observed of a point mass in a non-inertial system, with the Levenberg–Marquardt’s and Gauss–Newton algorithms for parameters optimisation is treated. The trajectories obtained are in good agreement with theoretical predictions. This shows that even the theoretical solution of an abstract problem typical for theoretical mechanics can be accompanied by effective experimental verification and computational optimisation. In order to compare the two optimisation methods, we will give an explanation of each method’s steps.

The mathematical model of the point mass in rotating system

Recall that Newton’s second law applies specifically in inertial frames, in fact, in exactly those frames for which the first law holds; therefore, definitely not in rotating axes. This means that it is usually best to use frames related by Galilean transformations. Sometimes, it is far more convenient to do the calculations in a

non-inertial frame. In such cases, the thing to do is to apply the second law in an inertial frame and then transform to the non-inertial frame.

We consider a turntable is rotating about the OZ_1 axis with an angular velocity ω . Let k_1 be a unit vector along the axis.

$R_1(O_1, x_1, y_1, z_1)$ is the coordinates of the rotating reference frame and $R(O, x, y, z)$ is the coordinates of an inertial reference frame (Figure 2).

On the rotating reference frame (assuming negligible friction), a point mass (M) with mass m and gravity centre G moves freely in a horizontal plane.

The basic equation in Newtonian mechanics: $F = m \cdot a^{in}$, a^{in} is the acceleration relative to the inertial frame. Alternatively, the forces apply on the point mass as seen by an observation co-moving with non-inertial system (Arya, 1990; Bligh, Ferebee, & Hughes, 1982):

$$m\vec{\gamma}(M/R_1) = \vec{R} + \vec{P} - \underbrace{2m \cdot \vec{\omega}(R_1/R) \wedge \vec{V}(M/R_1)}_{\text{Coriolis force}} - \underbrace{m \cdot \vec{\omega}(R_1/R) \wedge [\vec{\omega}(R_1/R) \wedge \vec{O}_1G]}_{\text{Centrifugal force}} \tag{1}$$

$$\vec{O}_1G = x_1\vec{i}_1 + y_1\vec{j}_1 \tag{2}$$

It is not that the physics dealt with Newtonian mechanics cannot be analysed in a non-inertial frame, but that the form of the equations of motion is different.

The other terms on the right-hand side are the Coriolis and centrifugal forces (Arya, 1990; Bligh et al., 1982).

The velocity in the rotating reference frame is the function of the point mass position:

$$\vec{V} = \dot{x}_1 \vec{i}_1 + \dot{y}_1 \vec{j}_1 \tag{3}$$

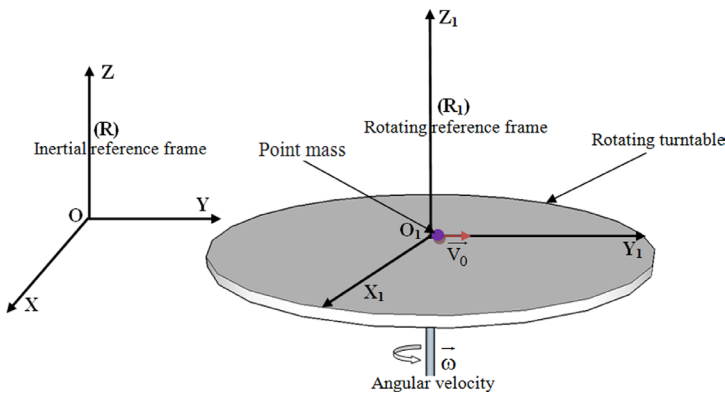


Figure 2. The scheme of the problem.

The Coriolis force is proportional to the rotation rate and the centrifugal force is proportional to its square. The Coriolis force acts in a direction perpendicular to the rotation axis and to the velocity of the body in the rotating reference systems (Boyd & Raychowdhury, 1981; McIntyre, 2000; Persson, 2000a). The centrifugal force acts outwards in the radial direction and is proportional to the distance of the body from the axis of the rotating reference systems. Equation (1) is a mathematical representation of what is meant by the statement that Newton's second law does not apply in a non-inertial reference frame.

Acceleration in the rotating reference frame is the function of the position of the point mass:

$$\vec{\gamma}(M/R_1) = \ddot{x}_1 \vec{i}_1 + \ddot{y}_1 \vec{j}_1 \quad (4)$$

The expression for differential equations of motion in the rotating reference frame can be written and decomposed into x_1, y_1 as follows:

$$m \cdot \ddot{x}_1 - 2 \cdot m \cdot \omega \cdot \dot{y}_1 - m \cdot \omega^2 \cdot x_1 = 0 \quad (5)$$

$$m \cdot \ddot{y}_1 + 2 \cdot m \cdot \omega \cdot \dot{x}_1 - m \cdot \omega^2 \cdot y_1 = 0 \quad (6)$$

Initial coordinates are:

$$x_1(0) = x_{10}, y_1(0) = y_{10}$$

$$\dot{x}_1(0) = \dot{x}_{10}, \dot{y}_1(0) = \dot{y}_{10}$$

The x_1 and y_1 coordinates specify the position of the point mass as seen by an observer on rotating frame.

Differential equations of motion seen below can be described by the system of coupled equations. The following is an analytic solution of the point mass in the rotating frame system, using a change of variable (complex number).

$$Z = x_1 + Iy_1 \quad (7)$$

Multiply the Equation (5) by I and add the Equation (6).

$$\ddot{x}_1 + I\ddot{y}_1 + 2\omega I(\dot{x}_1 + I\dot{y}_1) - \omega^2(x_1 + Iy_1) = 0 \quad (8)$$

The initial coordinates are:

$$x(0) + Iy(0) = (x_{10} + Iy_{10})$$

$$\dot{x}_1(0) + I\dot{y}_1(0) = (\dot{x}_{10} + I\dot{y}_{10})$$

The auxiliary variable Z occurs naturally in the unique differential equation as follows:

$$\ddot{Z} + 2\omega \cdot I \cdot \dot{Z} - \omega^2 Z = 0 \quad (9)$$

with:

$$Z(0) = Z_0$$

$$\dot{Z}(0) = \dot{Z}_0$$

The solution for Z is well known, the final expression is of the form:

$$Z(t) = Z_0 \cdot (1 + \omega \cdot I \cdot t) \cdot \exp(-I \cdot \omega \cdot t) + V_0 t \exp(-I \cdot \omega \cdot t) \quad (10)$$

Differential equations of motion can be described by the system of coupled equations. The analytical solution for differential equations of the rotating system in term of $x_1(t)$ and $y_1(t)$ is as follows (Haddout, Rhazi, & EL kenikssi, 2014):

$$\begin{aligned} x_1(t) &= (x_{10} - y_{10} \cdot \omega \cdot t + v_{x0} \cdot t) \cdot \cos(\omega \cdot t) + (y_{10} + x_{10} \cdot \omega \cdot t + v_{y0} \cdot t) \cdot \sin(\omega \cdot t) \\ y_1(t) &= (y_{10} + x_{10} \cdot \omega \cdot t + v_{y0} \cdot t) \cdot \cos(\omega \cdot t) + (-x_{10} + y_{10} \cdot \omega \cdot t - v_{x0} \cdot t) \cdot \sin(\omega \cdot t) \end{aligned} \quad (11)$$

where x_{10} and y_{10} is the initial position vector of launch, ω is the angular velocity, v_{x0} and v_{y0} is the initial condition of point mass launch.

Algorithms explanation

The non-linear least squares problem is closely related to the problem of solving a non-linear system of equations, and is a special case of the general optimisation problem in R^n (Häußler, 1983). Suppose that M data points (t_m, y_m) , $m = 1, 2 \dots M$, are fitting into a model $\psi(t; p)$ that depends on the parameter vector $p = (p_1, p_2, \dots p_k)^T$ (the superscript T denotes matrix transposition). The least squares method finds its optimum by minimising the objective function: (Häußler, 1983; Transtrum & Sethna, 2012; Wang, Cai, Zhu, Huang, & Zhang, 2015):

$$\begin{aligned} \min F(p) &= \min \sum_{m=1}^M r_m^2(p) \\ &= \min \sum_{m=1}^M (\psi(t_m; p) - y_m)^2 = \min \|r(p)\|^2 = \min r^T(p) \cdot r(p) \end{aligned} \quad (12)$$

where $r_m(p)$ stands for the error between the model $\psi(t; p)$ and the data y_m , $r(p) = (r_1(p), r_2(p), \dots r_k(p))^T$ is the error vector and $\|r(p)\|$ stands for the norm

of the vector $r(p)$. It is well known that when $\psi(t; p)$ is linear with the parameter p , Equation (12) is referred to as a linear least squares problem, otherwise a non-linear least squares problem.

If $\psi(t; p)$ is non-linear with the parameter p , Equation (12) is referred to as a linear least squares problem. Newton’s method is the fundamental method for non-linear least squares problem. Suppose that the function $r(p)$ has continuous derivative of second order, its Hessian matrix $\nabla^2 r(p)$ is positive definite and has explicit expression. Suppose that have the j^{th} trial parameter $p^{(j)}$, the target function $r(p)$ is approximated by a quadratic from of the Taylor series as follows (Wang et al., 2015):

$$r(p) \approx \zeta(p) = r(p^{(j)}) + [\nabla r(p^{(j)})]^T (p - p^{(j)}) + \frac{1}{2} \cdot (p - p^{(j)})^T \nabla^2 r(p^{(j)}) (p - p^{(j)}) \quad (13)$$

Set

$$\nabla \zeta(p) = \nabla r(p^{(j)}) + \nabla^2 r(p^{(j)}) (p - p^{(j)}) = 0 \quad (14)$$

Then

$$\nabla^2 r(p^{(j)}) (p - p^{(j)}) = -\nabla r(p^{(j)}) \quad (15)$$

If the Hessian matrix $\nabla^2 r(p^{(j)})$ is positive definite, $[\nabla^2 r(p^{(j)})]^{-1}$ exists. Then, the Newton’s method can be written as:

$$p^{(j+1)} = p^{(j)} - [\nabla^2 r(p^{(j)})]^{-1} \cdot \nabla r(p^{(j)}) \quad (16)$$

The $(j + 1)^{\text{th}}$ trial parameter $p^{(j+1)}$ is the new approximation of the minimum point of the function $r(p)$.

The beauty of Newton’s method is in its universality and fast convergence. However, if the function $r(p)$ only has first derivatives, the Newton’s method is not applicable to solve the minimisation problem. Then, the solution of the non-linear least squares problem can be approximated by one of the linear least squares problems through linearisation of the function $r(p)$. Set

$$\begin{aligned} \theta_m(x) &= r_m(p^{(j)}) + [\nabla r_m(p^{(j)})]^T (p - p^{(j)}) \\ &= [\nabla r_m(p^{(j)})]^T \cdot p - \{[\nabla r_m(p^{(j)})]^T \cdot p^{(j)} - r_m(p^{(j)})\}, \end{aligned} \quad (17)$$

$$m = 1, 2, \dots, M,$$

where the right side is the linear terms of the Taylor series of the error $r_m(p)$ near the current point $p = p^{(j)}$. Then

$$\theta(p) = \sum_{m=1}^M \theta_m^2(p) \quad (18)$$

The target function $r(p)$ is approximated by $\theta(p)$, thus the minimum of $r(p)$ is estimated by the minimum of $\theta(p)$. Then the non-linear least squares problem can be transformed into a linear least squares problem as:

$$\min \theta(p) = \min \sum_{m=1}^M \theta_m^2(p) \quad (19)$$

Set the Jacobian matrix:

$$J(x) = \begin{bmatrix} [\nabla r_1(p)]^T \\ [\nabla r_2(p)]^T \\ \vdots \\ [\nabla r_M(p)]^T \end{bmatrix} = \begin{bmatrix} \frac{\partial r_1(p)}{\partial x_1} & \frac{\partial r_1(p)}{\partial x_2} & \cdots & \frac{\partial r_1(p)}{\partial x_p} \\ \frac{\partial r_2(p)}{\partial p_1} & \frac{\partial r_2(p)}{\partial p_2} & \cdots & \frac{\partial r_2(p)}{\partial p_p} \\ \vdots & \vdots & \vdots & \vdots \\ \frac{\partial r_M(p)}{\partial p_1} & \frac{\partial r_M(p)}{\partial p_2} & \cdots & \frac{\partial r_M(p)}{\partial p_p} \end{bmatrix} \quad (20)$$

And

$$S = \begin{bmatrix} [\nabla r_1(p^{(j)})]^T p^{(j)} - r_1(p^{(j)}) \\ [\nabla r_2(p^{(j)})]^T p^{(j)} - r_2(p^{(j)}) \\ \vdots \\ [\nabla r_M(p^{(j)})]^T p^{(j)} - r_M(p^{(j)}) \end{bmatrix} = J(p^{(j)})p^{(j)} - r^{(j)} \quad (21)$$

where $r^{(j)}$ stands for the vector $[r_1(p^{(j)}), r_2(p^{(j)}), \dots, r_M(p^{(j)})]^T$. Then Equation (18) can be written as:

$$\theta(p) = [J(p^{(j)}) \cdot p - S]^T [J(p^{(j)}) \cdot p - S] \quad (22)$$

And

$$[J(p^{(j)})]^T J(p^{(j)}) \cdot (p - p^{(j)}) = -[J(p^{(j)})]^T r^{(j)} \quad (23)$$

If $J(p^{(j)})$ is a column filled matrix, $[J(p^{(j)})]^T J(p^{(j)})$ is a symmetric positive definite matrix, and thus $\{[J(p^{(j)})]^T J(p^{(j)})\}^{-1}$ exists.

The Gauss–Newton method is obtained: a start with an initial guess $x^{(0)}$ for the minimum, the method proceeds by the iterations (Björck, 1996; Gavin, 2011; Gratton, Lawless, & Nichols, 2007; Wang et al., 2015).

$$p^{(j+1)} = p^{(j)} - [J(p^{(j)})]^T J(p^{(j)})^{-1} \cdot [J(p^{(j)})]^T r^{(j)} \quad (24)$$

where the increments is:

$$\Delta p^j = -[J(p^{(j)})]^T J(p^{(j)})^{-1} \cdot [J(p^{(j)})]^T r^{(j)} \quad (25)$$

Also, the assumption $M \geq N$ in the algorithm statement is necessary, as otherwise the matrix $J_r^T J_r$ is not invertible and the normal equations cannot be solved (at least uniquely). The Gauss–Newton algorithm can be derived by linearly approximating the vector of functions r_m .

From this, it is evident that the advantage of Gauss–Newton method over the standard Newton’s method is that it does not require calculation of the second-derivative matrix (Hessian matrix) but compute the approximate Hessian matrix $H = [J(p)]^T J(p)$. However, the matrix $H = [J(p)]^T J(p)$ may not be invertible, in which case the Gauss–Newton method does not work (Wang et al., 2015). This can be overcome by adding a damping factor λ to the approximate Hessian matrix:

$$G = H + \lambda I = [J(p)]^T J(p) + \lambda I \quad (26)$$

where λ is a damping factor; we will adjust it based on estimates of how close we are to a solution or adjusted at each iteration to assure a reduction in the error ε .

Where I is the identity matrix. To make this matrix invertible, suppose that the eigenvalues and eigenvectors of $H = [J(p)]^T J(p)$ are $[\mu_1, \mu_2, \dots, \mu_p]$ and $[z_1, z_2, \dots, z_p]$. Then

$$Gz_m = [H + \lambda I]z_m = Hz_m + \lambda z_m = \mu_m z_m + \lambda z_m = (\lambda + \mu_m)z_m \quad (27)$$

Therefore, the eigenvectors of G are the same as the eigenvectors $H = [J(p)]^T J(p)$, and the eigenvalues of G are $(\lambda + \mu_m)$.

The matrix G can be made positive definite by increasing λ until $(\lambda + \mu_m) > 0$ for all m , and therefore G will be invertible. This leads *the Levenberg–Marquardt algorithm* (Marquardt, 1963; Ranganathan, 2004)

$$p^{(j+1)} = p^{(j)} - [J(p^{(j)})]^T J(p^{(j)}) + \lambda^{(j)}]^{-1} \cdot [J(p^{(j)})]^T r^{(j)} \quad (28)$$

This method adaptively varies the parameter updates between the gradient descent update and the Gauss–Newton update. Also, the method adjusts λ by either multiplying or dividing it by a small constant scaling factor δ on each step. A typical δ might be between 2 and 10 (Schwartz, 2008).

Where small values of the algorithmic parameter λ result in a Gauss–Newton update and large values of λ result in a gradient descent update. The parameter λ is initialised to be large. If an iteration happens to result in a worse approximation, λ is increased. As the solution approaches the minimum, λ is decreased, the Levenberg–Marquardt’s method approaches the Gauss–Newton method, and the solution typically converges rapidly to the local minimum (Gavin, 2011; Lourakis, 2005; Madsen, Nielsen, & Tingleff, 2004; Marquardt, 1963).

Model simulation of the different types of motion

The simulation results $y_1(x_1)$ (Equation 11) show the effect of inertial forces (assuming negligible friction). Figures 3 and 4 above are in function of the effect

of the extreme sensitivity of the trajectories in a rotating reference system, the initial conditions of launch point mass $V_0 = (V_{x0}, V_{y0})$, the angular velocity ω and initial position vector of launch (x_{10}, y_{10}) .

- Effect of the initial position (x_{10}, y_{10}) and direction of launch $V_0 = (V_{x0}, V_{y0})$
- We fix $\omega = 0.9 \text{ rad/s}$, $(x_{10}, y_{10}) = (0, -1)$ and $V_0 = (V_{x0}, V_{y0})$ such as: $V_0 = (-0.9, 0.57)$, $V_0 = (-0.57, 0.9)$ and $V_0 = (-0.9, 0.9)$ (Figure 3(a)). Also, $(x_{10}, y_{10}) = (0, -1)$, $(x_{10}, y_{10}) = (0, 1)$, $(x_{10}, y_{10}) = (1, 0)$, $(x_{10}, y_{10}) = (-1, 0)$ (Figure 3(b)).
- We fix $\omega = 0.9 \text{ rad/s}$, and $V_0 = (V_{x0}, V_{y0})$ such as: $V_0 = (0, -0.9)$, $V_0 = (0, -0.6)$ and $V_0 = (0, -1.15)$ (Figure 3(c)).
- Effect of initial velocity of launch $V_0 = (V_{x0}, V_{y0})$
- We fix $\omega = 0.5 \text{ rad/s}$, $(x_{10}, y_{10}) = (0, 0)$ and $V_0 = (V_{x0}, V_{y0})$ such as: $V_0 = (0, 0.1)$, $V_0 = (0, 0.4)$ and $V_0 = (0, 0.6)$, $V_0 = (0, 0.04)$ (Figure 4(a)).
- Effect of angular velocity ω
- We fix $(x_{10}, y_{10}) = (0, 0)$ and $V_0 = (0, 0.6)$ such as: $\omega = 0.2 \text{ rad/s}$, $\omega = 0.6 \text{ rad/s}$ and $\omega = 1.5 \text{ rad/s}$ (Figure 4(b)).

The results show, that all motions will be reduced outwards, with the right, the degree of deflection determined by the motion relative to the rotating turntable. The difference between the deflections constitutes the Coriolis effect (Persson, 2000a). For some angles of launch, a path has portions where the trajectory is

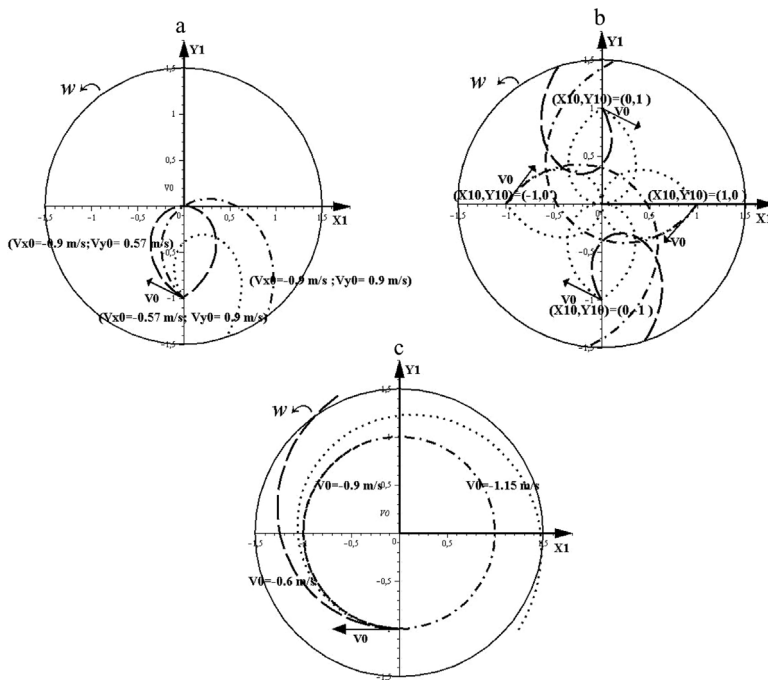


Figure 3. Spatial trajectory simulation, initial position and direction of launch effect (X_{10}, Y_{10}) , (V_{x0}, V_{y0}) (a, b, c) in a rotating frame.

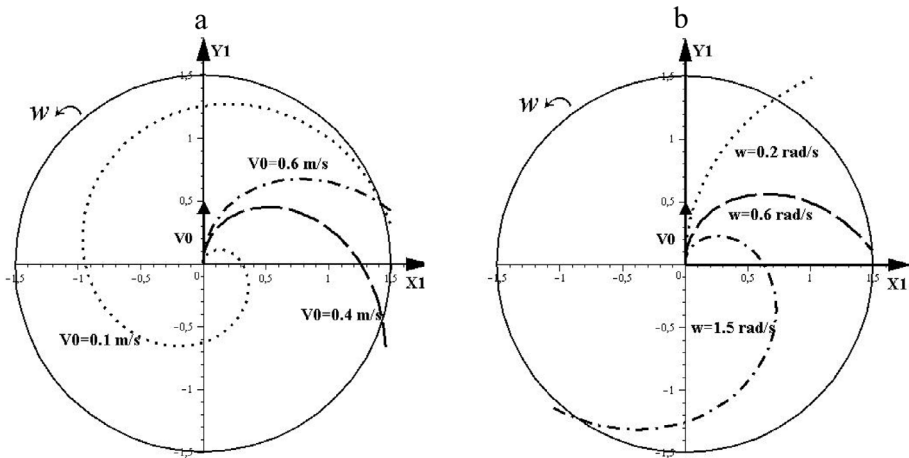


Figure 4. Spatial trajectory simulation, initial velocity and angular velocity effect (V_0 , ω) (a, b) in a rotating frame.

approximately radial, and Coriolis force is primarily responsible for the apparent deflection of the point mass (centrifugal force is radial from the centre of rotation, and causes little deflection on these segments). When a path curves away from radial, however, centrifugal force contributes significantly to deflection.

On the other hand, it is noted that the radius of curvature of the trajectory decreases with increasing the angular velocity (Figure 4(b)) and decreases with the initial velocity (Figure 4(a)). Additionally, it is possible to obtain the different situations in rotating system, for example: if the vector of launch is perpendicular on axis (y), the motion is circular (Figure 3(c)), also, if the vector of launch is angled on (y) axis, the motion is elliptical (Figure 3(a)).

Theory and experiment compared

Parameters optimisation of motion in a rotating system based on Levenberg–Marquardt and Gauss–Newton methods

A brief description of iterative algorithms (i.e. L–M and G–N) for parameters identification used in a rotating system.

It is desired to find a curve (model function) of the form:

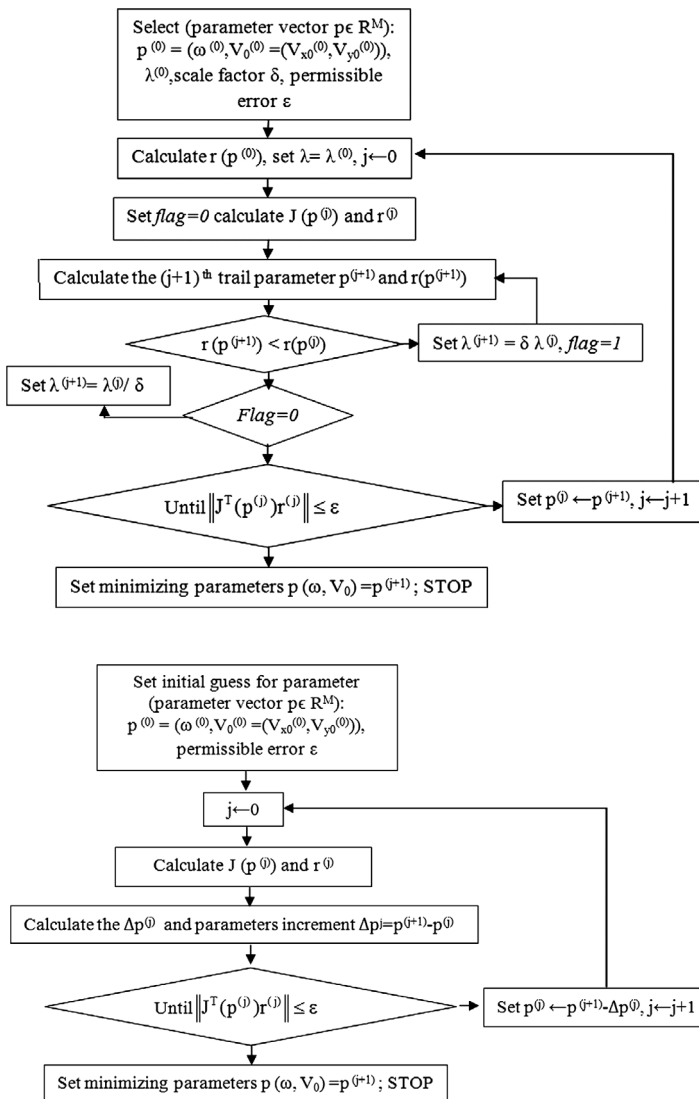
$$\begin{aligned}
 x_1(t) &= (x_{10} - y_{10} \cdot \omega \cdot t + v_{x0} \cdot t) \cdot \cos(\omega \cdot t) + (y_{10} + x_{10} \cdot \omega \cdot t + v_{y0} \cdot t) \cdot \sin(\omega \cdot t) \\
 y_1(t) &= (y_{10} + x_{10} \cdot \omega \cdot t + v_{y0} \cdot t) \cdot \cos(\omega \cdot t) + (-x_{10} + y_{10} \cdot \omega \cdot t - v_{x0} \cdot t) \cdot \sin(\omega \cdot t)
 \end{aligned}
 \tag{29}$$

Starting with the initial estimates of V_0 and ω , after 5 iterations of the Gauss–Newton algorithm and 10 iterations of the Levenberg–Marquardt algorithm, the optimal values V_0 and ω are obtained. The plot in the Figure 5 shows the curve

determined by the model for the optimal parameters vs. the observed data: effect of angular velocity, initial velocity and direction of launch. Comparisons of the field data with computed trajectory are summarised in Table 1. Our experimental results are in good agreement with theoretical calculations.

On the whole, it can be said that the model fitting of the motion in rotating frame performs well in representing the field data and a good estimation of parameters optimisation.

Note that the experimental arrangement was designed to be inexpensive (see Appendix 1). Hence, although better results for the problem surely could be obtained, we can declare that the agreement of theoretical calculations with the experimental data is very satisfactory.



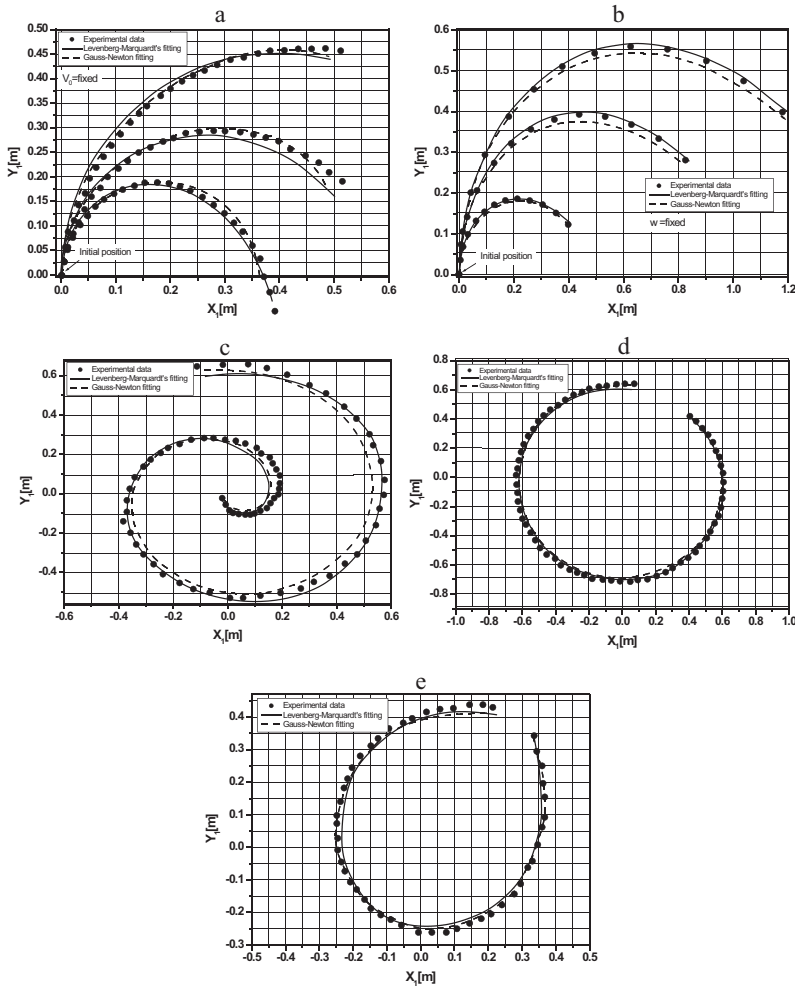


Figure 5. Field data and model computed spatial trajectory, showing initial velocity, angular velocity effect (V_0 , ω) (a, b), initial position and direction of launch effect (X_{10} , Y_{10} , V_{x0} , V_{y0}) (c, d, e) in a rotating reference frame.

Error analysis and algorithms comparisons

Non-linear least squares problem are an incredibly useful tool for analysing sets of data and determining whether or not a mathematical model is a good fit for data obtained experimentally. Although it involves the solving of a system of non-linear equations, it provides us with a powerful, rapidly converging tool that provides answers to a system of equations that does not have an absolute solution. We have shown, in our problem that given a system that does have a known solution, the Gauss–Newton and Levenberg–Marquardt’s methods will provide the correct answer. There are drawbacks to the Gauss–Newton method, such as the fact that it will not converge if the initial guesses are not in a suitable range; however, it is nonetheless a powerful computational tool that provides answers where analytic methods fail. However, the Levenberg–Marquardt’s method finds a solution even if it starts very far from the

Table 1. Comparison of algorithms/experimental data with different condition.

Rotating frame situations	Angular velocity fixed (rad/s)	Initial velocity varied (m/s)	Initial velocity fixed (m/s)	Angular velocity varied (rad/s)	Elliptical Trajectory (rad/s); (m/s)	Circular trajectory (rad/s); (m/s)	Spiral trajectory (rad/s); (m/s)
Experimental data	$\omega = 1.50$	$V_1 = 0.50$ $V_2 = 1.05$ $V_3 = 1.50$	$V_0 = 0.83$	$\omega_1 = 2.15$ $\omega_2 = 1.44$ $\omega_3 = 1.11$	$V_0 = 0.96$ $\omega = 2.08$	$V_0 = 0.96$ $\omega = 2.08$	$V_0 = 0.3$ $\omega = 1.28$
Levenberg–Marquardt’s	$\omega = 1.50$	$V_1 = 0.50$ $V_2 = 1.08$ $V_3 = 1.51$	$V_0 = 0.79$	$\omega_1 = 2.09$ $\omega_2 = 1.45$ $\omega_3 = 1.06$	$V_0 = 0.93$ $\omega = 2.01$	$V_0 = 0.93$ $\omega = 1.95$	$V_0 = 0.27$ $\omega = 1.25$
Gauss–Newton	$\omega = 1.52$	$V_1 = 0.48$ $V_2 = 1.03$ $V_3 = 1.48$	$V_0 = 0.80$	$\omega_1 = 2.10$ $\omega_2 = 1.48$ $\omega_3 = 1.07$	$V_0 = 0.93$ $\omega = 1.98$	$V_0 = 0.93$ $\omega = 1.86$	$V_0 = 0.23$ $\omega = 1.23$

Table 2. Error statistical indicators of the two algorithms.

Algorithms	ω fixed (SD %; RMSE)	$V_i(i=1..3)$ varied (V_i (SD %; RMSE))	V_0 fixed (SD %; RMSE)	$\omega_i(i=1..3)$ varied (ω_i (SD %; RMSE))	Elliptical Trajectory (V_0, ω)	Circular trajectory (V_0, ω)	Spiral trajectory (V_0, ω)
L–M	(0; 0)	V_1 (0.7%; 0.0070) V_2 (1.1%; 0.012) V_3 (0.1%; 0.0022)	(3.9; 0.0460)	ω_1 (0.8%; 0.0078) ω_2 (0.9%; 0.0360) ω_3 (0.6%; 0.0057)	(0.3%; 0.0024)	(0.3%; 0.0021)	(0.2%; 0.0027)
G–N	(0.2; 0.0036)	V_1 (2.2%; 0.029) V_2 (2.2%; 0.021) V_3 (1.6%; 0.015)	(3.7; 0.0480)	ω_1 (2.9%; 0.0375) ω_2 (0.7%; 0.0042) ω_3 (0.5%; 0.0058)	(0.3%; 0.0023)	(0.3%; 0.0024)	(0.3%; 0.0030)

final minimum. On the other hand, the robustness of Levenberg–Marquardt’s and Gauss–Newton algorithms is tested using statistical indicators (standard deviation (SD) and root mean square error (RMSE)), see Table 2 for each condition value.

At a large distance from the function minimum, the steepest descent method is utilised to provide steady and convergent progress towards the solution. As the solution approaches the minimum, damping parameter λ is adaptively decreased, the Levenberg–Marquardt’s algorithm approaches the Gauss–Newton algorithm, and the solution typically converges rapidly to the minimum (Gavin, 2011; Madsen et al., 2004; Wang, Mi, Su, & Zhao, 2012).

Conclusion

This study aims to understand the rotating frame of reference and the inertial force through some analyses that are conducted on the parameters in a rotating frame. Also, the two algorithms Levenberg–Marquardt’s and Gauss–Newton for parameters optimisation of the motion observed of a point mass in a non-inertial reference frame in Newtonian mechanics are used. The obtained experimental results are in good agreement with the theory. Moreover, it turns out that the study

of such theoretically rather complicated (but also realistic) problems can be very instructive for physics education, when accompanied by a simple quantitative experimental verification. On the other hand, an optimal value has been demonstrated in this study. In addition, the algorithms' accuracy of parameters optimisation using statistical test has been evaluated, shows Levenberg–Marquardt's algorithm is more robust than Gauss–Newton algorithm at small error values. Using algorithms methods for parameters optimisation in Newtonian mechanics can help problem study in practical and theoretical physics.

In the other hand, the knowledge and skills studied separately in the courses of mechanics, theoretical mechanics, optimization methods, computational software, laboratory measurements and measurements processing for analysing and solution of particular real-world mechanical problems (i.e. the explanation of many phenomena in connection with the winds and currents of the ocean ... etc).

Disclosure statement

No potential conflict of interest was reported by the authors.

References

- Agha, A., Gupta, S., & Joseph, T. (2015). Particle sliding on a turntable in the presence of friction. *American Journal of Physics*, 83, 126–132.
- Arya, A. P. (1990). *Introduction to classical mechanics* (p. 73). Boston, MA: Allyn and Bacon.
- Bard, Y. (1970). Comparison of gradient methods for the solution of nonlinear parameter estimation problems. *SIAM Journal on Numerical Analysis*, 7, 157–186.
- Björck, A. (1996). *Numerical methods for least squares problems*. Philadelphia, PA: SIAM.
- Bligh, P. H., Ferebee, I. C., & Hughes, J. (1982). Experimental physics with a rotating table. *Physics Education*, 17, 89–94.
- Boyd, J. N., & Raychowdhury, P. N. (1981). Coriolis acceleration without vectors. *American Journal of Physics*, 49, 498–499.
- Costa, L. F. O., & Natário, J. (2015). Inertial forces in general relativity. *Journal of Physics: Conference Series*, 600, 012053. IOP Publishing. doi:<http://dx.doi.org/10.1088/1742-6596/600/1/012053>
- Gavin, H. (2011). *The Levenberg-Marquardt method for non-linear least squares curve-fitting problems* (pp. 1–15). Department of Civil and Environmental Engineering, Duke University, Durham, NC, USA.
- Gratton, S., Lawless, A. S., & Nichols, N. K. (2007). Approximate Gauss–Newton methods for nonlinear least squares problems. *SIAM Journal on Optimization*, 18, 106–132.
- Haddout, S., Maslouhi, A., & Igouzal, M. (2015). Predicting of salt water intrusion in the Sebou river estuary (Morocco). *Journal of Applied Water Engineering and Research*, 1–11.
- Haddout, S., Rhazi, M., & EL kenikssi, M. (2014). Study of the inertia forces conception and realization a device experimental pedagogical. *International Journal of Innovation and Applied Studies*, 8, 673–684.
- Häußler, W. M. (1983). A local convergence analysis for the Gauss-Newton and Levenberg-Morrison-Marquardt Algorithms. *Computing*, 31, 231–244.
- Kim, J, Kido, H, Rangel, R. H., & Madou, M. J. (2008). Passive flow switching valves on a centrifugal microfluidic platform. *Sensors and Actuators B: Chemical*, 128, 613–621.

- Kirkpatrick, L., & Francis, G. (2009). *Physics: A conceptual world view* (7th ed.). Pacific Grove, CA: Cengage Learning/Thomson Brooks/Cole. p. 653.
- Lourakis, M. I. (2005). *A brief description of the Levenberg-Marquardt algorithm implemented by levmar*. Heraklion, Crete, Greece: Foundation of Research and Technology.
- Madsen, K., Nielsen, N. B., & Tingleff, O. (2004). *Methods for non-linear least squares problems* (Technical Report). Lyngby: Informatics and Mathematical Modeling, Technical University of Denmark.
- Marquardt, D. W. (1963). An algorithm for least-squares estimation of nonlinear parameters. *Journal of the Society for Industrial & Applied Mathematics*, 11, 431–441.
- McIntyre, D. H. (2000). Using great circles to understand motion on a rotating sphere. *American Journal of Physics*, 68, 1097–1105.
- Persson, A. (2000a). Back to basics: Coriolis: Part 1 - What is the Coriolis force? *Weather*, 55, 165–170.
- Persson, A. (2000b). Back to basics: Coriolis: Part 3 - The Coriolis force on the physical earth. *Weather*, 55, 234–239.
- Persson, A. (2000c). Back to basics: Coriolis: Part 2 - The Coriolis force according to Coriolis. *Weather*, 55, 182–188.
- Ranganathan, A. (2004). The Levenberg-Marquardt algorithm. *Tutorial on LM Algorithm*, 1–5.
- Schwartz, R. (2008). *Biological modeling and simulation: A survey of practical models, algorithms, and numerical methods*. Cambridge, MA and London, England: MIT Press.
- Simuunek, J., & Hopmans, J. W. (2000). Parameter optimization and non-linear fitting. In J. H. Dane & G. C. Topp (Eds.), *Methods of Soil Analysis, Part 1, Physical Methods* (pp. 139–157), Chapter 1.7, (3rd ed.), Madison, WI: SSSA.
- Taylor, K. (1974). Weight and centrifugal force. *Physics Education*, 9, 357–360.
- Transtrum, M. K., & Sethna, J. P. (2012). Improvements to the Levenberg-Marquardt algorithm for nonlinear least-squares minimization. arXiv preprint arXiv:1201.5885. Cornell University, USA.
- Wagner, A., Altherr, S., Eckert, B., & Jodl, H. J. (2006). Multimedia in physics education: A video for the quantitative analysis of the centrifugal force and the Coriolis force. *European Journal of Physics*, 27, 27–30. doi:<http://dx.doi.org/10.1088/0143-0807/27/5/L01>
- Wang, S., Cai, G., Zhu, Z., Huang, W., & Zhang, X. (2015). Transient signal analysis based on Levenberg–Marquardt method for fault feature extraction of rotating machines. *Mechanical Systems and Signal Processing*, 54–55, 16–40.
- Wang, F., Mi, Z., Su, S., & Zhao, H. (2012). Short-term solar irradiance forecasting model based on artificial neural network using statistical feature parameters. *Energies*, 5, 1355–1370.
- Yeh, W. W.-G. (1986). Review of parameter identification procedures in groundwater hydrology: The inverse problem. *Water Resources Research*, 22, 95–108.

Appendix A. Experimental device (rotating frame used in this study)

